Measurement 99 (2017) 7–12

Contents lists available at ScienceDirect

Measurement

journal homepage: www.elsevier.com/locate/measurement

Electroluminescence of silicon solar cells using a consumer grade digital camera

M. Frazão [a], J.A. Silva [b,*], K. Lobato [b], J.M. Serra [b]

[a] Faculdade de Ciências, Universidade de Lisboa, Portugal
[b] Instituto Dom Luiz, Faculdade Ciências, Universidade Lisboa, Portugal

ARTICLE INFO

Article history:
Received 6 September 2016
Received in revised form 5 December 2016
Accepted 6 December 2016
Available online 8 December 2016

Keywords:
Characterization
Solar cells
Electroluminescence imaging
Defect detection

ABSTRACT

Electroluminescent imaging is increasingly used to detect defects in silicon solar cells. However, the cost of the conventional luminescence systems is a limiting factor for generalized use. A simple and reliable low-cost electroluminescence setup is presented. The developed system was tested on commercial silicon solar cells for the acquisition of electroluminescence images in the forward and reverse bias regimes. In forward bias the temperature was varied whilst in reverse bias the applied voltage was varied. The results used in conjunction allowed for the detection of defective areas and identification of their type and cause.

The simplicity and low-cost nature of the developed setup should enable a more widespread use of luminescence techniques for the characterization of crystalline silicon solar cells.

1. Introduction

Imaging techniques are essential tools in photovoltaic research as they allow for the collection of spatially resolved information of a solar cell's electrical and optical response [1]. Electroluminescence (EL) is one of the most popular imaging methods for the characterization of silicon solar cells and modules. The major advantages of EL are its simplicity and ability to produce high resolution mappings using short acquisition times, which also allow for it to be applied in industrial settings as in-line characterization tool.

For PV grade Si under normal working conditions the Shockley-Read-Hall (SHR) recombination mechanism [2,3] is dominant and determines device performance. This results from intra-bandgap transitions mediated by defects in the crystal lattice or impurities. The result is that areas with a high defect density will have a low minority carrier density.

Although radiative recombination is negligible for solar cell functioning under normal working conditions, its magnitude is dependent on minority carrier densities and as such its detection provides information on minority carrier densities even if dominated by the SHR recombination. Radiative recombination results from direct band-to-band transitions of an electron from lower energy levels of the conduction band to the higher energy levels in the valence band. The energy released as a photon is equal to this transition (between 1.45 eV/850 nm and 1.08 eV/1150 nm) and as such is detectable by a Si-CCD sensor. The typical spectral sensitivity of Si-CCD sensors is characterized by a maximum between 500 and 800 nm with a subsequent decay to zero into the near infrared (ca. 1050 nm).

Fuyuki et al. [4] first proposed electroluminescence imaging as a method to perform a photographic survey of the solar cell minority carriers' diffusion lengths. The principle of electroluminescence measurement is very simple, the solar cell is injected with a current in forward bias and the band-to-band electron-hole radiative recombination is imaged. Further developments followed such as the mapping of diffusion lengths by taking the ratio of two images obtained with different spectral filters [5] or the mapping of the cell's local series resistance [6].

Similar reports also followed whereby the carrier injection was achieved not by applying a bias but by illumination [4,5,7]. This has the advantage that characterization can be performed from bare wafers all the way to finished solar cells. However, because such systems require the use of high powered lasers, sophisticated means of filtering out the stray laser light and more sensitive sensors, their cost is significantly higher hindering widespread use.

The combination of EL with another imaging technique (lock-in thermography) was shown to provide complimentary information on the solar cell local properties [8].

* Corresponding author.
E-mail address: jose.silva@fc.ul.pt (J.A. Silva).

http://dx.doi.org/10.1016/j.measurement.2016.12.017
0263-2241/

In recent years Reverse Bias Electroluminescence (ReBEL) method has become a common tool for the characterization of silicon solar cells [9,10]. During ReBEL characterizations the solar cells are inversely polarized with voltages between 2 and 16 V, inducing high currents in the solar cells. In contrast to EL, ReBEL imaging is based on the acceleration and subsequent scattering or recombination of charge carriers in high electric fields [11] and as such areas of high luminescence are the defective areas. It has been shown that ReBEL characterization not only allows for the detection of solar cell voltage breakdowns, but also permits their identification [11,12]. Type-1 voltage breakdowns occur at biases $|V| < 9$ V and are mostly observed in edge regions of a solar cell. Typically this type of breakdown is related to surface contaminations with metals (e.g. Al). For this type of breakdown there is no visible correlation with the forward-bias EL image. Type-2 voltage breakdowns occur between |9| V and |12| V. This breakdown is related to recombination-active crystal defects, possibly due to the presence of lattice dislocations or metallic contaminations in the bulk. In this case there is a good correlation with the EL image. Type-3 breakdowns are observed for biases greater than $|V| > 13$ V and as such are at times referred to as "avalanche-break downs". This type of breakdown is caused by etch-pits or other sharp kinks in the lattice near the p-n junction.

EL and ReBEL are now usually used in conjunction as these techniques provide complementary information by detection of broken fingers, bulk contamination, dislocations, cracks and surface problems.

The defects that affect solar cell performance can be considered as intrinsic or extrinsic [13]. Intrinsic defects are due to inherent material properties (e.g. surface and interface recombination), while extrinsic defects are mainly due to processing defects (e.g. wafer cracks, broken fingers). Another interesting feature of EL characterization is that the luminescence response of intrinsic defects is more sensitive to temperature variation than extrinsic defects. Therefore by performing EL measurements at different temperatures, a clear distinction between intrinsic and extrinsic defects can be established [13].

In this article a low cost electroluminescence system developed in our laboratory is presented and its proficiency in EL and ReBEL imaging of Si solar cells demonstrated. The system is based on the use of a consumer grade digital camera. The cost of such a camera is approximately an order of magnitude smaller than a scientific grade camera. As such, this type of setup should therefore enable a wider spread of use even for example in PV teaching laboratories.

2. Electroluminescence setup

The electroluminescence system developed is presented in Fig. 1. The system is comprised of a light-tight black-box where housed inside is a digital camera and a sample holder. The digital camera is equipped with a standard F-mount 18–55 mm lens. To allow for detection in the near infrared, the IR filter was removed and replaced with a full spectrum window of equal optical path length. In our setup a Nikon D40 was used, but in principle any digital camera with similar grade CCD or CMOS sensor and where the IR filter can be removed would serve the purpose.[1] Also for higher resolution cameras, the signal-to-noise ratio can be improved at the expense of some loss of spatial resolution by combining adjacent pixels in one (i.e. binning). The sample holder is made of Al and temperature controlled whereby the temperature is monitored by an embedded thermocouple and regulated by water flow. The sample holder also has a vacuum system to ensure optimal electrical and thermal contact between the sample holder and the back contact of the solar cell. The sample holder allows for the placement of samples of varying sizes up to the standard 156×156 mm^2. The bias was applied and the resultant current measured by a voltage/source meter. A 4-point contact setup was used to remove the contact resistance influence which can be significant for high currents. Since the acquisition times used are much longer than the automatic maximum acquisition time allowed by the camera software, the camera was operated in bulb mode; here the shutter remains open whilst the shutter release button is pressed and thus allows for arbitrary shutter opening times and thus acquisition times. Since the camera is inside the light-tight box the shutter activation must be remotely activated. To do this, one can use different strategies[2]; in our set up a pneumatic piston activated by nitrogen pressure was used to pressure the shutter button. Since the objective of luminescence imaging is to establish a clear distinction between brighter and darker areas, all the images acquired were obtained by setting the camera to Black & White mode.[3] The images were captured in the Nikon Electronic Format ".nef" which is a RAW image format. The images were then converted to ".TIF" format for processing. During the first tests a dark measurement (i.e. zero bias) of the solar cell EL was performed and subtracted to the EL image. But since no significant difference was detected between the as captured measurement and the corrected one, and once the study of the solar cell EL images performed is mainly qualitative, it was decided to simplify the procedure, presenting the as captured luminescence image.

3. Experimental procedure

For EL image acquisition a bias of +0.6 V was applied between the front and back contacts resulting in currents of ca. 1 A. In this case and for the samples in question, the optimum acquisition time was set to 6 min. This allows for full dynamic range use of the sensor without saturating it.

For ReBEL image acquisition the biases were varied between −4 V and −18 V. Once again, to ensure full dynamic range use of the sensor, the acquisition time was set to 15 min.

To validate the identification of defective areas of the imaged solar cells, these were further characterized by measuring internal quantum efficiency (IQE) and evaluating the minority diffusion length [14].

In order to distinguish the intrinsic material defects from the extrinsic ones, EL images of solar cells were obtained at two different temperatures and subsequently subtracted to obtain a difference image.

[1] The removal of the IR filter is not specific to the camera used here. Also this practice is not endorsed by camera manufacturers. However, this process is widely available in speciality camera repair & modification companies. The modification can be performed on a wide range of currently available consumer grade digital cameras from point-and-shoot to entry level DSRLs to professional grade DSLRs.

[2] For several commercial cameras there are remote controls available on the market that allow the use of long acquisition times in a simple and straightforward way. That was not the case for the Nikon D40 used.

[3] By setting the camera to form Black & White images, the camera's software examines the RGB values of each pixel and through propriety algorithms sets of all these to an equal value resulting in a grey scale. The sensor in the Nikon D40 camera has a RGBG Bayer pattern colour filter array where for every red and green sensing pixel there are two green pixels so as to more closely match human eye sensitivity. Nonetheless, the colour filter array is not 100% blocking of IR photons and, as such, in an environment where there is in principle no photons in the visible spectrum, a portion of IR photons penetrate the colour filter array to arrive at the pixel for detection. The use of a colour filter array in consumer cameras is almost ubiquitous for the formation of colour images. If it were removed then the camera would be transformed into a monochrome camera with the upside of becoming more sensitive because photons are not lost by absorption the colour filter array. However, this modification is complex as it requires physically detaching the colour filter array from the sensor surface.

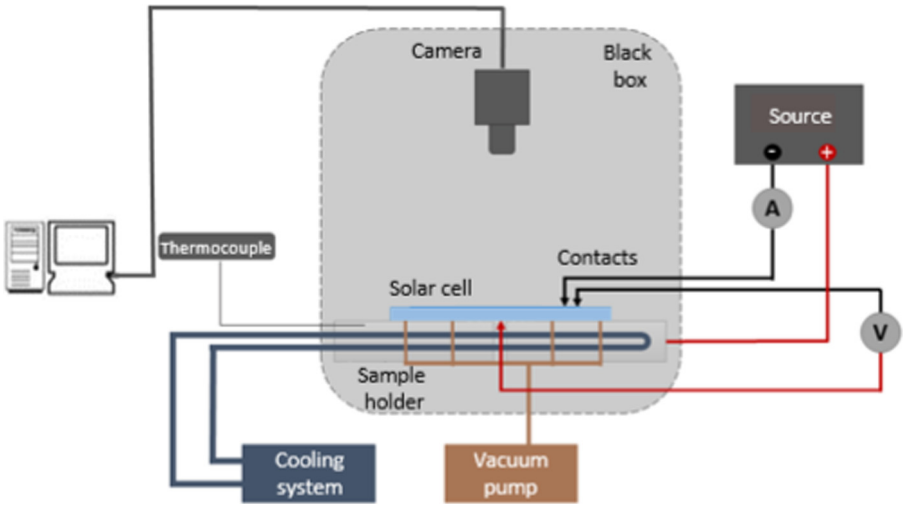

Fig. 1. Electroluminescence experimental setup [15].

4. Solar cell characterization

4.1. Electroluminescence imaging

Before starting the solar cells characterization, it was verified that the acquisition setup worked adequately. Fig. 2 shows the EL images of two monocrystalline solar cells. Two types of defects are forthrightly observed: in Fig. 2(a) the bright/dark regions are indicative of the existence of contact grid problems, namely broken fingers; in Fig. 2(b) a cross-shaped defect near the center of the solar cell (marked as A) is indicative of a crack. Also, a dark region is visible at the lower-right corner of the solar cell (marked as B), which is indicative of the existence of a high recombination region (either due to bulk or surface defects). It is worth stating that none of the mentioned defects could be detected by visual inspection of the solar cells.

Fig. 3(a) and (b) shows the EL and ReBEL image of two multicrystalline silicon solar cells. In the EL images the grain-boundaries, which are regions of higher carrier recombination, are easily identified as dark lines. Also for both solar cells, regions of higher recombination can be distinguished: the identified area in the EL image of solar cell 1, Fig. 3(a), can be attributed to the presence of crystal grain boundaries were the SRH recombination is particularly high, possibly due to presence of a high concentration of metallic dopants or lattice dislocations; the area identified in the EL image of solar cell 2, Fig. 3(b), the presence of a region with dark spots near the margin is indicative of a higher contamination regions, possibly due to a substrate contamination during ingot growth, or a problem occurred during solar cell processing such as an inhomogeneous emitter formation.

4.2. ReBEL imaging

The ReBEL characterization of the two multicrystalline solar cells are also shown in Fig. 3(c) and (d). There is a good correlation between the EL and ReBEL images of the respective cells, namely in the marked areas. For solar cell 1, Fig. 3(c), one can observe the same high recombination area previously highlighted and can also be correlated to several high recombination grain boundaries. Because these areas begin to manifest when the applied bias is $V = -12$ V, this suggests that the defects in these areas are associated to type-2 voltage breakdowns, i.e. due to recombination-active crystal defects. For the encircled region this is most likely due to a bulk metallic contamination, for the grain-boundaries the cause is most likely the high density of crystal dislocations.

For solar cell 2, Fig. 3(c), the correlation exists for the region marked in at one of the margins. At $V = -12$ V this is a type-2 breakdown, and because of the distribution of observed defects, this suggests the presence of a metallic contamination.

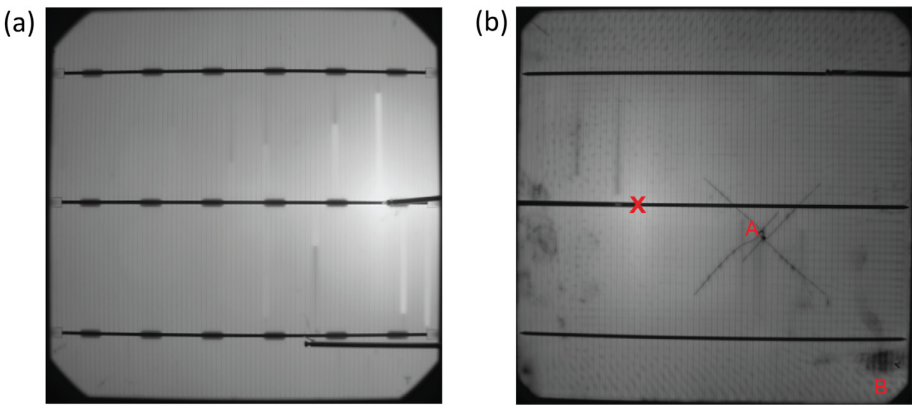

Fig. 2. Electroluminescence imaging of two monocrystalline silicon solar cells.

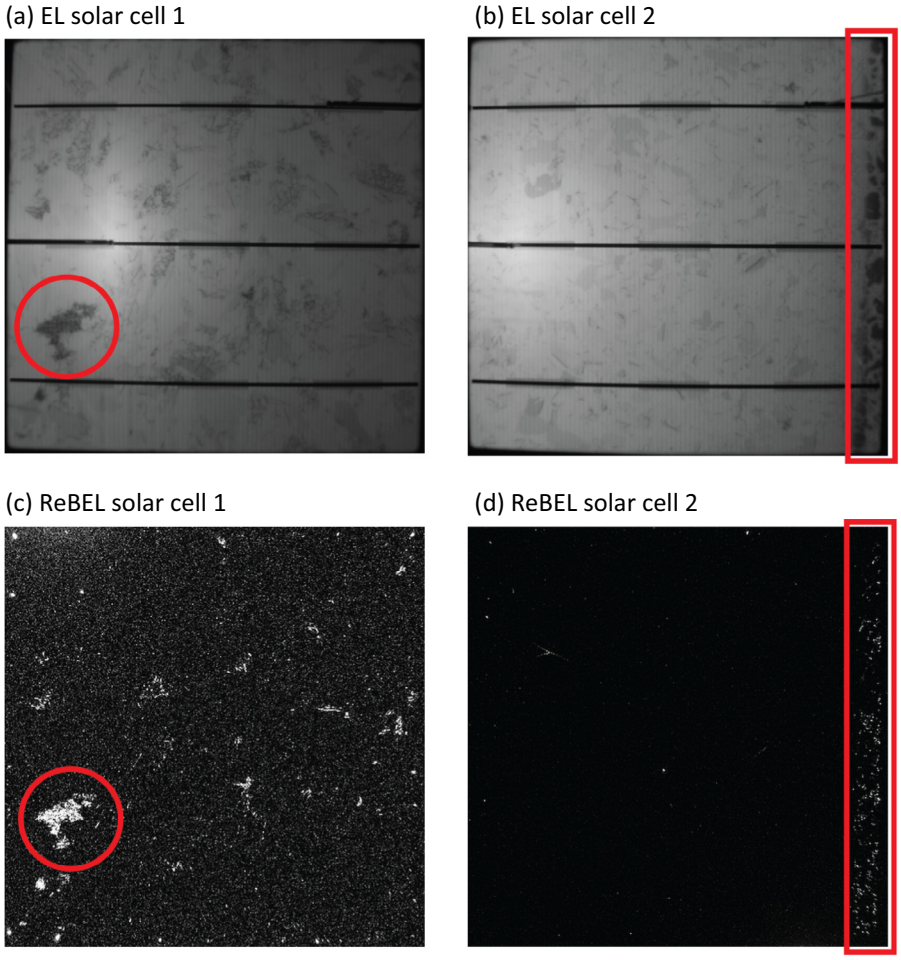

Fig. 3. EL and ReBEL imaging of two multicrystalline silicon solar cells. The red boundaries indicate areas of high recombination. (For interpretation of the references to colour in this figure legend, the reader is referred to the web version of this article.)

Other sporadic spots are observed in the ReBEL image of solar cell 2 begin to manifest themselves at lower biases (i.e. type-1 breakdown) and do not correlate with the EL image. As such, these are probably due to metallic contamination of the surface of the solar cell, most likely aluminum.

4.3. EL reponse compared to IQE response

Shown in Fig. 4(a) is an EL image acquired for a section of the solar cell presented in Fig. 3(a). The two differing areas selected for IQE measurements are identified as being normal and defective.

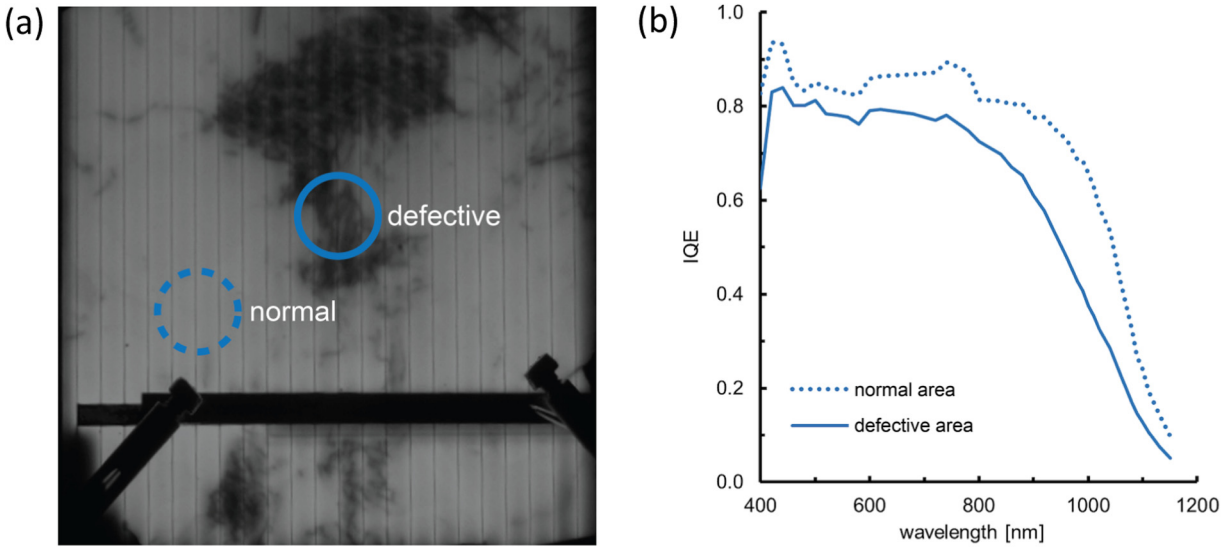

Fig. 4. (a) EL image of bottom left hand section (4×4 cm^2) of solar cell shown in Fig. 3(a) and identification of the selected normal and defective areas. (b) IQE measurements at the two respective areas.

Table 1
Diffusion lengths for the points characterized.

Point	Le (μm)
Normal	110
Defective	475

The IQE of the two areas is shown in Fig. 4(b). The curve corresponding to the darker EL area is lower in magnitude throughout and in particular begins to decay at shorter wavelengths (800 nm vs. 950 nm). Analysis of the IQE confirms that there is significant difference in the minority diffusion length L_e (see Table 1) hence a higher carrier recombination rate.

An analogous study was performed for the monocrystalline solar shown in of Fig. 2(b) with similar results, suggesting the existence of a region with high bulk recombination (i.e. low L_e) on the lower right hand corner, possibly due to a local metal contamination.

4.4. Intrinsic and extrinsic defects

To further investigate the nature of defects, EL images of a multicrystalline silicon solar cell were obtained at two different temperatures and the resulting images subtracted (see Fig. 5).

The EL images were analyzed in more detail by graphing a section of the EL images and are shown in Fig. 6. The first observation is that the EL signal increases gradually to a peak and then decreases. The peak corresponds to the point closest to current injection and is due to the luminescence signal being dependent on the local voltage [5]. Due to current flow there is always a voltage drop in the bus-bar and fingers. However, this variation is no longer observed in the resultant subtraction image.

This dependence of the absolute value of EL does not jeopardize the defect analysis performed, since this analysis is essentially based on relative variations of the EL signal. For instance, even if the EL signal has a clear bias, the presence of defects A and B can be unambiguously identified in the EL image obtained at 22 °C. Nevertheless, to achieve higher accuracy in EL imaging, current injection via multiple-point contact probes should be considered.

The luminescence signal of extrinsic defects, e.g. crack signaled marked as A, are less sensitive to temperature variations and as such the subtraction results in a smaller difference (darker regions in the subtraction image). Such defects are particularly emphasized in EL measurements at high temperatures when the effect of extrinsic ones weaken. By closer inspection of the EL signal and difference (see Fig. 6) one can observe that there is almost no variation in signal intensity at the two temperatures (i.e. the difference signal is almost 0).

The brighter regions of the subtraction image, e.g. area marked as B, are areas where the luminescence signal has varied the most with temperature. These correspond to intrinsic bulk defects essentially associated to grain-boundaries. By observing closely the EL signal and difference (see Fig. 6) one can observe that the subtraction signal has a marked increase.

5. Conclusions

An electroluminescence setup based on consumer grade digital camera was developed. The acquisition EL and ReBEL images on both monocrystalline and multicrystalline silicon solar cells showed that the detection of differing types of defects in solar cells is possible, i.e., contact grid problems, grain-boundary related dislocations and metal contaminations. Also, the identification of

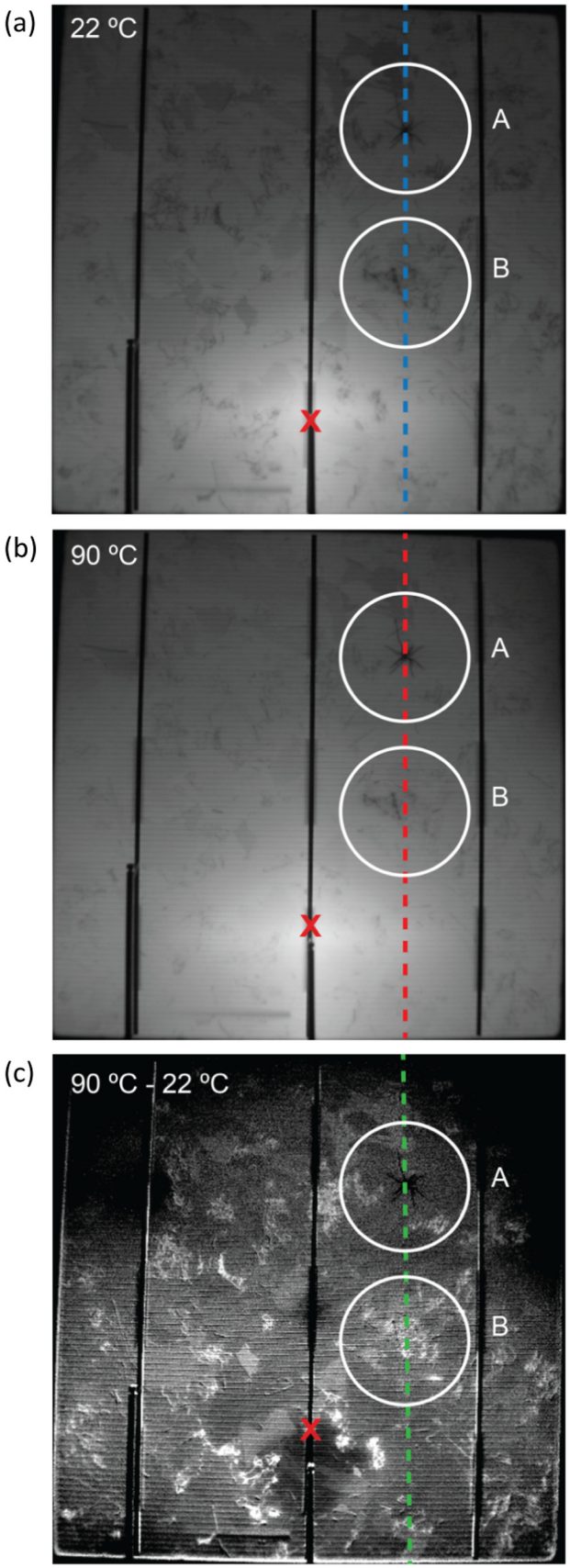

Fig. 5. EL images of a multicrystalline silicon solar cell at: (a) 22 °C; and (b) 90 °C; (c) resulting substraction image, the dotted lines correspond to the sections graphed in Fig. 6.

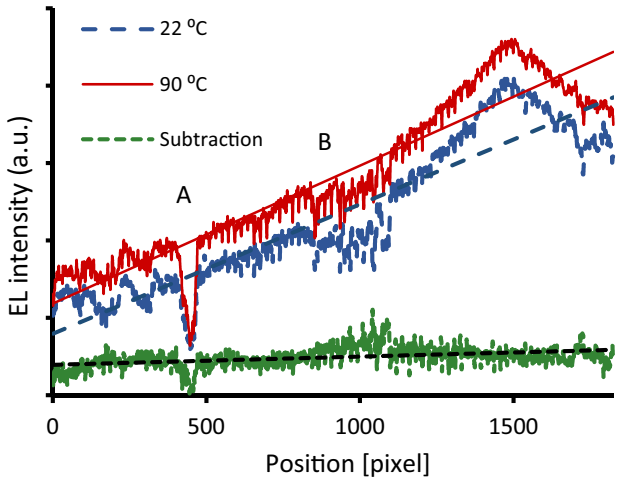

Fig. 6. Variation of the EL signal along a line of a multicrystalline solar cell. Pixel position is counted from the top of the individual images shown in Fig. 5. The trendlines are linear fits by least squares method.

defect areas was also confirmed by independent measurements of the local diffusion length. EL measurements were also performed at different temperatures allowing for the distinction between intrinsic and extrinsic defects.

Current injection at a single point was shown to introduce some artifacts into the acquired EL images. As such, multiple-point contacts should be employed to reduce this effect.

As the developed system proved its ability as a low-cost system for EL and ReBEL image acquisition of solar cells, it is possible to envisage the widespread use of similar systems in module inspection by small and medium sized PV system installers or even in physics and engineering undergraduate and postgraduate PV courses.

Acknowledgements

This work has been funded by FCT (Portugal) through the grant SFRH/BPD/82540/2011 and by the project FCT: PESTOE/CTE/LA0019/2013.

References

[1] T.C.M. Müller, B.E. Pieters, T. Kirchartz, R. Carius, U. Rau, Effect of localized states on the reciprocity between quantum efficiency and electroluminescence in Cu(In, Ga)Se_2 and Si thin-film solar cells, Sol. Energy Mater. Sol. Cells 129 (2014) 95–103.
[2] W. Shockley, W.T. Read, Statistics of the recombinations of holes and electrons, Phys. Rev. 87 (1952) 835.
[3] R.N. Hall, Electron-hole recombination in germanium, Phys. Rev. 87 (1952) 387.
[4] T. Fuyuki, H. Kondo, T. Yamazaki, Y. Takahashi, Y. Uraoka, Photographic surveying of minority carrier diffusion length in polycrystalline silicon solar cells by electroluminescence, Appl. Phys. Lett. 86 (2005) 262108.
[5] P. Würfel, T. Trupke, T. Puzzer, E. Schäffer, W. Warta, S.W. Glunz, Diffusion lengths of silicon solar cells from luminescence images, J. Appl. Phys. 101 (2007) 123110.
[6] D. Hinken, K. Ramspeck, K. Bothe, B. Fischer, R. Brendel, Series resistance imaging of solar cells by voltage dependent electroluminescence, Appl. Phys. Lett. 91 (2007) 182104.
[7] T. Kirchartz, A. Helbig, W. Reetz, M. Reuter, J.H. Werner, U. Rau, Reciprocity between electroluminescence and quantum efficiency used for the characterization of silicon solar cells. Progress in photovoltaics: research and applications, 1, Prog. Photovoltaics Res. Appl. 17 (2009) 394–402.
[8] K. Ramspeck, K. Bothe, D. Hinken, B. Fischer, J. Schmidt, R. Brendel, Recombination current and series resistance imaging of solar cells by combined luminescence and lock-in thermography, Appl. Phys. Lett. 90 (2007) 153502.
[9] D. Lausch, K. Petter, H.V. Wenckstern, M. Grundmann, Correlation of pre-breakdown sites and bulk defects in multicrystalline silicon solar cells, Phys. Status Solidi – Rapid Res. Lett. 3 (2009) 70–72.
[10] K. Bothe, K. Ramspeck, D. Hinken, C. Schinke, J. Schmidt, S. Herlufsen, R. Brendel, J. Bauer, J.M. Wagner, N. Zakharov, O. Breitenstein, Luminescence emission from forward- and reverse-biased multicrystalline silicon solar cells, J. Appl. Phys. 106 (2009) 104510.
[11] O. Breitenstein, J. Bauer, K. Bothe, W. Kwapil, D. Lausch, U. Rau, J. Schmidt, M. Schneemann, M.C. Schubert, J.M. Wagner, W. Warta, Understanding junction breakdown in multicrystalline solar cells, J. Appl. Phys. 109 (2011) 071101.
[12] D. Lausch, K. Petter, R. Bakowskie, C. Czekalla, J. Lenzner, H. von Wenckstern, M. Grundmann, Identification of pre-breakdown mechanism of silicon solar cells at low reverse voltages, Appl. Phys. Lett. 97 (2010) 073506.
[13] T. Fuyuki, A. Kitiyanan, Photographic diagnosis of crystalline silicon solar cells utilizing electroluminescence, Appl. Phys. A 96 (2009) 189–196.
[14] R.T. Swimm, K.A. Dumas, Optical absorption coefficient and minority carrier diffusion length measurements in low-cost silicon solar cell material, J. Appl. Phys. 53 (1982) 7502–7504.
[15] M. Frazão, Electroluminescência de células solares, Master Dissertation Faculdade de Ciências Universidade de Lisboa, 2016.